SLAC-PUB-6024 Rev.
CU-TP-582
April 1993
(T)

High Energy Quark-Antiquark Elastic Scattering with Mesonic Exchange[1]

Wai-Keung Tang

Stanford Linear Accelerator Center

Stanford University, Stanford, CA 94309

Abstract

We studied the high energy elastic scattering of quark anti-quark with an exchange of a mesonic state in the t channel with $-t/\Lambda^2 \gg 1$. Both the normalization factor and the Regge trajectory can be calculated in PQCD in cases of fixed (non-running) and running coupling constant. The dependence of the Regge trajectory on the coupling constant is highly non-linear and the trajectory is of order of 0.2 in the interesting physical range.

(Submitted to *Physical Review* **D**)

[1]Work supported in part by Department of Energy contract DE-AC03-76SF00515.

1 Introduction

With the advances of LHC and SSC, it is possible to study experimentally the Regge behavior in the parton level where the momentum transfer squared $-t \gg \Lambda^2$ but is still smaller than the center of mass energy squared s of the partons. The Regge limit of the parton scattering amplitudes corresponds to the small x limit of parton distribution, while the presence of a "large" scale $-t$ justifies the use of perturbative QCD.

The sea-quark and gluon distribution for small x is related to the Balitsky-Fadin-Kuraev-Lipatov (BFKL) Pomeron [1]. The distributions of sea-quarks and gluons grow like $x^{-\alpha_P}$ at small x. where α_P is the trajectory of the BFKL Pomeron. The behavior of the valence-quark distributions is controlled by the mesonic Reggeons [1]. It grows as $x^{-\omega_R}$ with ω_R the trajectories of the mesonic Reggeons. However, great care is necessary to separate the perturbative behavior from the non-perturbative soft physics.

Several hard partonic processes to measure the behavior of the BFKL Pomeron [2-7] have been discussed in the literature. In Ref [7], A.H. Mueller and the author proposed a process of high energy, fixed t parton-parton scattering through the exchange of a BFKL Pomeron. It is natural to extend this idea to the process whereby a mesonic Reggeon is exchanged. It is the objective of this paper to set up the necessary machinery to investigate the process of the mesonic Reggeon exchange and to study

the possibilty of measuring such behavior. The scattering amplitudes are calculated, while the normalization factor and the trajectory can be obtained explicitly.

In this paper, we study the quark anti-quark scattering amplitudes [Fig.1] with flavor exchange in the t channel. In the kinematic region,

$$s \simeq \mid u \mid \gg -t \simeq \mu^2 \gg \Lambda^2, \tag{1}$$

where the auxiliary parameter μ is the infrared cutoff of the transverse component of the momenta (with respect to the initial momenta p_1 and p_2) of virtual particles in the Feynman integrals where the terms $\sim \alpha(\mu^2)[(\alpha(\mu^2)/\pi)\ln^2(s/\mu^2)]^n$ are summed, and $\alpha(\mu^2)$ is the strong coupling constant at the scale μ^2. This is the double logarithmic (DL) approximation. The method of separating the softest virtual particle [8] allows one to calculate the partial wave amplitudes in the double logarithmic approximation. In Ref [9], R. Kirschner and L.N. Lipatov give equations for the partial wave of the amplitudes for both the color singlet and the octet exchange in the t channel. The octet exchange is suppressed, because it has a strong tendency to radiate gluons in the rapidity interval defined by the colliding quark anti-quark. This phenomenon is reflected by the negative intercept of the Regge trajectories of the octet exchange. In what follows, we restrict ourselves to the consideration of the color singlet exchange. Based on the partial wave results in Ref [9], we study in detail the scattering amplitudes for cases of both fixed (non-running) and running coupling constants, using analytic methods as far as possible.

The outline of the paper is as follows: In Sec. 2, we review the results of the partial wave amplitudes for the color singlet exchange. Scattering amplitudes for the fixed coupling case are presented in Sec. 3 for both positive and negative signature cases. In Sec. 4, both approximate and numerical methods are employed to study the effect of the inclusion of a running constant in the positive signature. Finally, Sec. 5 summarizes our conclusion.

2 Review of the partial wave amplitudes

We consider the amplitudes of annihilation ($q\overline{q} \to Q\overline{Q}$) with the exchange of a meson-like state in the t channel. With respect to the color group $SU(N)$, the amplitudes can be decomposed into a singlet $[M_0(s)]$ and an octet $[M_v(s)]$. In double-logarithmic approximation, the spinor structure of the Born term is preserved in higher order, so we can write the amplitudes as $b_0 M(s,t)$ where $b_0 = \gamma_\mu^\perp \otimes \gamma_\mu^\perp / s$ is the Born amplitude but without the coupling constant g^2. M_0 and M_v are

$$M_0 \mid_{Born} = \frac{N^2-1}{2N} g^2 \quad , \quad M_v \mid_{Born} = -\frac{1}{2N} g^2, \tag{2}$$

after using the color projectors P_0 (singlet) and P_v (octet)

$$P_{o\ ab}^{\ a'b'} = \frac{1}{N}\delta_{aa'}\delta_{bb'} \quad , \quad P_{v\ ab}^{\ a'b'} = \delta_{ab}\delta_{a'b'} - \frac{1}{N}\delta_{aa'}\delta_{bb'} \tag{3}$$

and the decomposition

$$M_{ab}^{a'b'} \;\; = \;\; P_{0\ ab}^{\ a'b'} M_0 + P_{v\ ab}^{\ a'b'} M_v \tag{4}$$

where $a,\ b$ and $a',\ b'$ label the color states of the initial and final quarks.

The asymptotics of the scattering amplitudes at large s and fixed t are determined by the singularities of the partial wave $f_j(t)$ in the crossed channel. In order to express the amplitude in terms of partial wave, we need to divide the amplitude $M_{0,v}$ into parts that are symmetrical and anti-symmetrical with respect to the transformation $s \leftrightarrow u \simeq -s$:

$$M^{\pm}(s) \;=\; \frac{1}{2}[M(s) \pm M(-s)]. \tag{5}$$

In double-logarithmic approximation, the Sommerfeld-Watson transformation reduces to the Mellin transformation, and the even (odd) part of the amplitude is related to the positive (negative signature) partial wave

$$M^p(s/\mu^2) \;=\; \int_{a-i\infty}^{a+i\infty} \frac{d\omega}{2\pi i} \xi^p(\omega) f^p(\omega) (\frac{s}{\mu^2})^{\omega}, \tag{6}$$

with $f^p(\omega)$ includes the factor $(sin\pi\omega)^{-1}$ usually written explicity in the Sommerfeld-Watson integral. The signature factor is given by

$$\xi^p(\omega) = \;\; \tfrac{1}{2}(e^{-i\pi\omega} + p) \;\simeq \begin{cases} 1 & p = +1 \\ -\frac{1}{2} i\pi\omega & p = -1 \end{cases}. \tag{7}$$

Using the method of isolating the softest virtual particle with the lowest transverse momentum $k_\perp^2$ in the Feynman diagrams, R. Kirschner and L.N. Lipatov were able to give equations for the partial wave amplitudes. The positive signature amplitudes

are

$$
\begin{aligned}
f_0^+(\omega) &= \frac{a_o g^2}{\omega} + \frac{1}{8\pi^2\omega}(f_0^+(\omega))^2, \text{and} \\
f_v^+(\omega) &= \frac{a_v g^2}{\omega} + \frac{b_v g^2}{8\pi^2\omega}\frac{d}{d\omega} f_v^+(\omega) + \frac{1}{8\pi^2\omega}(f_v^+(\omega))^2,
\end{aligned} \tag{8}
$$

while the negative signature amplitude is more complicated,

$$
f_0^-(\omega) = \frac{a_0 g^2}{\omega} - \frac{(N^2-1)g^2}{4\pi^2 N\omega} f_v^+(\omega) + \frac{1}{8\pi^2\omega}(f_0^-(\omega))^2 \tag{9}
$$

with

$$
a_0 = \frac{N^2-1}{2N}, \qquad a_v = -\frac{1}{2N}, \qquad b_v = N \tag{10}
$$

and boundary conditions

$$
f_i^+ \mid_{\omega\to\infty} = \frac{a_i g^2}{\omega} \qquad (i = 0, v). \tag{11}
$$

Here we list the partial wave amplitudes that are relevant to the color singlet exchange. The first terms in the above equations are the contribution from the Born terms which have pole singularity at $\omega = 0$.

The equations of color singlet exchange are purely algebraic, so that the solutions can be written in explicit form:

$$
\begin{aligned}
f_0^+(\omega) &= 4\pi^2\omega\,[\,1 - \sqrt{1-(\tfrac{\omega^+}{\omega})^2}\,] \\
f_0^-(\omega) &= 4\pi^2\omega\,[\,1 - \sqrt{1-(\tfrac{\omega^+}{\omega})^2(1-\tfrac{1}{2\pi^2\omega}f_v^+)}\,]
\end{aligned} \tag{12}
$$

which shows that $f_0^+(\omega)$ has a square-root branch point at (Fig.2)

$$\omega = \omega^+ = (\frac{g^2(N^2-1)}{4\pi^2 N})^{1/2} = (\frac{\alpha_s(N^2-1)}{\pi N})^{1/2}, \tag{13}$$

while $f_0^-(\omega)$ has singularity to the right of ω^+ so that it becomes dominant when energy is large. The equation for $f_v^+(\omega)$ is of Riccatti type. It can be solved easily and leads to the following result:

$$\begin{aligned} f_v^+(\omega) &= N g^2 \frac{d}{d\omega} \ln[\exp(\frac{1}{4}(\frac{\omega}{\omega_v})^2)\mathcal{D}_{p_v}(\frac{\omega}{\omega_v})] \\ \omega_v^2 &= \frac{g^2}{8\pi^2}N, \quad p_v = \frac{a_v}{b_v} = -\frac{1}{2N^2}, \end{aligned} \tag{14}$$

where $\mathcal{D}_\nu(z)$ is the parabolic-cylinder function [11].

In deriving $f_i(\omega)$, the coupling constant was taken to be fixed. But as the transverse momentum $k_\perp^2$ covers the large range from μ^2 to s [9], contribution from the running coupling is important and cannot be neglected. As demonstrated later, the inclusion of the running coupling constant changes the singularity of the partial wave amplitude from square root singularity to pole singularity.

Taking into account the effect of running coupling, the positive-signature singlet channel partial wave amplitude $F(\omega, \mu^2)$ satisfies

$$\mu^2 \frac{\partial}{\partial \mu^2} F(\omega,\mu^2) - \omega F(\omega,\mu^2) + \frac{1}{8\pi^2}(F(\omega,\mu^2))^2 + a_0 g^2(\mu^2) = 0 \tag{15}$$

with the boundary conditions

$$(\frac{\mu_0^2}{\mu^2})^\omega F(\omega,\mu^2)\mid_{\mu^2\to\infty} \to 0$$

$$F(\omega,\mu^2)\mid_{\omega\to\infty} \;\;\to\;\; \frac{a_0 g^2(\mu^2)}{\omega}. \tag{16}$$

The solution to the above equation is given by

$$F(\omega,\mu^2) \;\; = \;\; 8\pi^2\mu^2\frac{\partial}{\partial\mu^2}\ln[\Psi(-\frac{a_0}{8\pi^2 b\omega},0;\frac{\omega}{bg^2(\mu^2)})] \tag{17}$$

where $b=(\frac{11}{3}N-2/3N_f)/16\pi^2$, the coefficient of the first term of β function. $\Psi(a,c;z)$ is a confluent hypergeometric function [10] defined by

$$\Psi(a,c,z) \;\; = \;\; \frac{1}{\Gamma(a)}\int_0^\infty e^{-zt}t^{a-1}(1+t)^{c-a-1}dt. \tag{18}$$

3 Fixed coupling

For the positive signature channel,

$$M_0^+(s) \;\; = \;\; \int_{a-i\infty}^{a+i\infty}\frac{d\omega}{2\pi i}(\frac{-s}{t})^\omega f_0^+(\omega) \tag{19}$$

where we have set $\mu^2=-t$. Substituting $f_0^+(\omega)$ from eq. (12), we have

$$M_0^+(s) \;\; = \;\; \int_{a-i\infty}^{a+i\infty}\frac{d\omega}{2\pi i}(\frac{-s}{t})^\omega 4\pi^2\omega\;[1-\sqrt{1-(\tfrac{\omega^+}{\omega})^2}], \tag{20}$$

where the contour of integration is shown in Fig.2. We take the branch cut from $-\omega^+$ to $+\omega^+$, so the contour of integration can be deformed to encircle the branch cut. The positive signature amplitude becomes

$$M_0^+(s) \;\; = \;\; \int_{\omega^+}^{-\omega^+}\frac{d\omega}{2\pi i}\,(\frac{-s}{t})^\omega\;4\pi^2\omega\;\;\mathrm{Dis}\;[1-\sqrt{1-(\tfrac{\omega^+}{\omega})^2}]\;. \tag{21}$$

With Dis $[1-\sqrt{1-(\frac{\omega^+}{\omega})^2}] = 2i\frac{|\omega^{+\,2}-\omega^2|^{1/2}}{\omega}$ and modified Bessel function I_ν defined by

$$I_\nu(z) = \frac{(z/2)^\nu}{\Gamma(\nu+1/2)\Gamma(1/2)}\int_{-1}^{1}(1-t^2)^{\nu-1/2}e^{\pm zt}dt. \tag{22}$$

$M_0^+(s)$ is evaluated as

$$M_0^+(s) = \frac{(2\pi)^2\omega^+}{y}I_1(\omega^+ y) \tag{23}$$

where $y=\ln(s/-t)$, the rapidity interval between the quark anti-quark pair. If y is large, i.e. in the asymptotic region,

$$I_1(\omega^+ y) \simeq \frac{e^{\omega^+ y}}{\sqrt{2\pi\omega^+ y}}$$

and

$$M_{asy}^+(s) = \frac{(2\pi)^{3/2}\omega^{+\,2}}{(\omega^+ y)^{3/2}}e^{\omega^+ y} \tag{24}$$

which shows the Regge limit behavior.

As mentioned before, the negative signature channel dominates asymptotically, so an explicit solution is desired. However, because f_v^+ depends on the parabolic-cylinder function, it is not possible to have a convenient solution. In view of that, we take lim $N\to\infty$. The limit is not just an academic exercise but has its own significance, because the relevant parameter in this problem is $p_v=-1/2N^2=-1/18$ which can be taken to be zero without introducing much error. With [11]

$$\frac{d}{dz}(e^{z^2/4}\mathcal{D}_\nu(z)) = \nu e^{z^2/4}\mathcal{D}_{\nu-1}(z),$$

$f_v^+(\omega)$ can be rewritten as

$$f_v^+(\omega) \;=\; -\frac{1}{2N}\frac{g^2}{\omega_v}\frac{\mathcal{D}_{p_v-1}(\frac{\omega}{\omega_v})}{\mathcal{D}_{p_v}(\frac{\omega}{\omega_v})}. \tag{25}$$

In the limit, $p_v = -1/2N^2 \to 0$ while

$$\omega^{+\,2} = \frac{\alpha_s(N^2-1)}{\pi N} \to \frac{\alpha_s N}{\pi} = 2\omega_v^2. \tag{26}$$

With the help of [11],

$$\begin{aligned} \mathcal{D}_0(z) &= e^{-z^2/4}, \;\; \text{and} \\ \mathcal{D}_{-1}(z) &= \sqrt{\frac{\pi}{2}}\, e^{z^2/4}\, \mathrm{Erfc}(\tfrac{z}{\sqrt{2}}), \end{aligned} \tag{27}$$

where $\mathrm{Erfc}(z)$ is the complementary error function. $f_v^+(\omega)$ can be simplified as

$$f_v^+(\omega) \;=\; -\frac{2\pi^2\omega^+}{N^2}\, e^{(\frac{\omega^+}{\omega})^2}\, \mathrm{Erfc}(\tfrac{\omega^+}{\omega}). \tag{28}$$

Define $u = \frac{\omega^+}{\omega}$, and drop the first term of the negative partial wave amplitude in eq.(12) as it has no singularity and hence contributes nothing to the amplitudes after performing the Mellin transformation. $f_0^-(\omega)$ then reduces to

$$f_0^-(\omega) \;=\; -\frac{(2\pi)^2\omega^+}{u}\sqrt{u[u^3 - u - \frac{\pi^{1/2}}{N^2}\, e^{u^2}\mathrm{Erfc}(u)]}. \tag{29}$$

Expression (29) is corrected up to the order $1/N^2$ and clearly the correction term comes from $f_v^+(\omega)$. The zeros of the expression $u^3 - u - \frac{\pi^{1/2}}{N^2}\, e^{u^2}\, \mathrm{Erfc}(u)$ evaluated numerically are found to be $u_+ = 1.0388$ and $u_- = -0.4668$. As $u_+ > 1$, the square

root singularity of the negative channel lies to the right of that of the positive signature channel. But $u_+ - 1 = .0388$ is not large. This indicates that both channels have similar behavior phenomenologically. The expression $u^3 - u - \frac{\pi^{1/2}}{N^2} e^{u^2} \mathrm{Erfc}(u)$ can be approximated by $(u - u_+)(u - u_-)^2$ within the region $u_- \leq u \leq u_+$ which is chosen to be the branch cut. With this approximation,

$$f_0^-(\omega) \;=\; -\frac{(2\pi)^2 \omega^+}{u}(u - u_-)\sqrt{u(u - u_+)}. \tag{30}$$

Performing the Mellin tranformation by deforming the contour of integration to enclose the branch cut from $u = 0$ to $u = u_+$ (Fig. 3) leads to

$$\begin{aligned} M_0^-(s) &= \pi^2 (\omega^+)^3 \int_0^{u_+} du\, (\frac{-s}{t})^{\omega^+ u}\, (u - u_-)\;\; \mathrm{Dis}\sqrt{u(u - u_+)} \\ &= 2i\pi^2 (\omega^+)^3 \int_0^{u_+} du\, (\frac{-s}{t})^{\omega^+ u}\, (u - u_-) \mid u(u - u_+) \mid^{1/2}. \end{aligned} \tag{31}$$

Change variable u' to $u - u_+/2$, and the integral can be expressed in terms of the modified Bessel function I_ν,

$$\begin{aligned} M_0^-(s) &= i\frac{\pi^3 \omega^{+\,2}}{y}\, e^{u_+ \omega^+ y/2}\;\; [(\frac{u_+}{2} - u_- - \frac{2}{\omega^+ y}) I_1(u_+ \omega^+ y/2) \\ &\quad + \frac{u_+}{2} I_0(u_+ \omega^+ y/2)]. \end{aligned} \tag{32}$$

In the asymptotic region where y is large, the amplitude reduces to

$$M_{asy}^-(s) \;=\; \frac{i\sqrt{2}}{4}\pi(u_+ - u_-)\, \omega^+\, e^{(u_+ - 1)\omega^+ y}\;\; M_{asy}^+(s) \tag{33}$$

with $M_{asy}^+(s)$ given by eq. (24). In the range of SSC energies where $y \sim 8$ and

$\omega^+ \sim 0.5$,

$$\frac{\sqrt{2}}{4}\pi(u_+ - u_-)\ \omega^+\ e^{(u_+-1)\omega^+ y} \quad \sim \quad 1, \tag{34}$$

which suggests that the positive and negative signature amplitudes are of the same order and cannot be distinguished in the interesting energies range. Actually, y needs to be about 50 before the negative signature channel is appreciatively different from the positive signature channel. The difference between $\sqrt{2}\omega_v$ and ω^+ in eq. (26) enhances the negative signature channel a little bit. Effectively, it changes $u_+ - 1 = 0.0388$ to 0.1, but its effect is still small at SSC energies.

The two amplitudes have a phase difference of $\sim \pi/2$, because $M^+_{asy}(s)$ is purely real while $M^-_{asy}(s)$ is purely imaginary, and they have nearly the same magnitude. Both give a non-linear quark anti-quark Regge trajectory $\omega(t) \sim \sqrt{\alpha_s(-t)}$.

4 Running Coupling

As we have already mentioned, there is reason to believe that the inclusion of running coupling effects will greatly change the behavior of the amplitudes. In this section, we would like to restrict ourselves to the study of the positive signature singlet channel. It is plausible to suggest that the inclusion of the running coupling effect would not change the similarity between the positive and negative signature amplitudes greatly for the following reasons: the only difference between the positive and negative chan-

nels stems from the contribution of the double logarithmic soft gluon; the soft gluon contributes to the negative signature singlet channel but not the positive signature singlet channel [9]. However, as seen in the previous section, the soft gluon does not change the amplitude appreciatively. The inclusion of the running coupling will decrease the importance of the soft gluon contribution as the coupling between quark and gluon is smaller than in the fixed coupling case. Therefore, for practical purposes, we can take positive and negative singlet amplitudes to be equal in magnitude but with phase difference $\pi/2$.

In the following subsections, we will study the effect of the running coupling in the positive signature channel using two different methods. In the first method, we take $\lim b \to 0$, where b is the coefficient of the first term in the β function. In this approximation, we will recover the previous $f_0^+(\omega)$ result with a correction term which is liner in b. However, as we will show later, the correction term enhances the amplitude by $(\ln y)^{3/2}$ relative to the $f_0^+(\omega)$ term, so that the correction term dominates asymptotically and the approximation breaks down. The breakdown of b expansion in the asymptotic region closely relates to the fact that the transverse momentum in the loop integral extends to the order of s. It illustrates that in the asymptotic region, the running coupling effect is not a small perturbation to the fixed coupling, but rather, it changes the behavior of the amplitudes dramaically.

In the second method, we take the approximation $\lambda = a_0/(8\pi^2 b\omega) \to \infty$. It gives

a fairly accurate result with $\sim 10\%$ error compared to the numerical calculation, even though the value of λ lies between 1 and 2 when the running coupling constant is in the interesting physical range.

Let us define

$$\lambda = \frac{a_0}{8\pi^2 b\omega}, \qquad \nu = \frac{\omega}{g^2(\mu^2)b}. \tag{35}$$

Both λ and ν are positive if $\omega > 0$. In the color singlet channel, the trajectories lie to the right of the origin of the complex ω plane, because the higher order diagrams enhance the amplitudes. This is in contrast to the case of the color octet exchange which suppresses the amplitude. It is safe to assume that both λ and ν are positive. As Ψ's dependence on μ^2 is through the running coupling constant $g^2(\mu^2)$, it is better to write

$$\frac{\partial}{\partial\mu^2} = \mu^2\frac{\partial g^2}{\partial\mu^2} = \omega\frac{\partial}{\partial\nu} \tag{36}$$

where $\mu^2\frac{\partial g^2}{\partial\mu^2} = -bg^4$. In terms of λ and ν, the partial wave amplitude $F(\omega,\mu^2)$ is

$$F(\omega,\mu^2) \;=\; 8\pi^2\omega\frac{\partial}{\partial\nu}\ln[\Psi(-\lambda,0;\nu)]. \tag{37}$$

4.1 b expansion

In the limit $b\to 0$, $\lambda,\nu\to\infty$; Ψ can be approximated by [10]

$$\begin{aligned}\Psi(-\lambda,0;\nu) \;&=\; \lambda^\lambda\nu^{1/4}(\nu-4\lambda)^{-1/4} \\ &\quad \exp(-\lambda+\frac{\nu}{2}-\frac{1}{2}\nu^{1/2}(\nu-4\lambda)^{1/2}+\lambda\ln[\tfrac{(\nu^{1/2}+(\nu-4\lambda)^{1/2})^2}{4\lambda}])\end{aligned} \tag{38}$$

which leads to

$$\frac{\partial}{\partial\nu}\ln[\Psi(-\lambda,0;\nu)] \;=\; \frac{1}{2}[1-(1-\frac{4\lambda}{\nu})^{1/2}-\frac{2\lambda}{\nu(\nu-4\lambda)}]. \tag{39}$$

The second term in the above expression turns out to be independent of b and with the first term, it recovers $f_0^+(\omega)$. The third term, which is the correction term, is found to be

$$\frac{2\lambda}{\nu(\nu-4\lambda)} \;=\; \frac{2\pi b\alpha_s{\omega^+}^2}{\omega(\omega^2-{\omega^+}^2)}. \tag{40}$$

It is linear in b and has a pole singularity at $\omega=\omega^+$ in contrast to the square root singuarity of the first term. Putting eqs. (37), (39), and (40) together, we get

$$F(\omega) \;=\; f_0^+(\omega)-\frac{(2\pi)^3 b\alpha_s{\omega^+}^2}{\omega^2-{\omega^+}^2}. \tag{41}$$

The negative sign of the correction terms indicates that the running coupling reduces the overall amplitude. This behavior is also found in the Pomeron exchange [4]. The contribution of the correction term to the positive signature amplitude is

$$\Delta M_0^+(s) \;=\; -\frac{(2\pi)^3}{2}b\alpha_s\omega^+\, e^{\omega^+ y} \tag{42}$$

which leads, in the asymptotic region, to

$$\begin{aligned} M_{run}^+ &= M_0^+ + \Delta M_0^+ \\ &= [1-(2\pi)^{1/2}\pi b\alpha_s\omega^+ y^{3/2}]M_{asy}^+ \end{aligned} \tag{43}$$

where the correction term has $y^{3/2}$ dependence relative to the first order term. The approximation is valid only when

$$(2\pi)^{1/2}\pi b\alpha_s\omega^+ y^{3/2} \ll 1.$$

With $\omega^+ \sim 0.4$, $\alpha_s \sim 0.20$ and $b = 0.053$ (four flavors), the above inequality implies $y \ll 9.7$ which is the boundary of the asymptotic region.

4.2 $\lambda \to \infty$ approximation

Before taking any approximation, let us study the nature of the singularity of the partial wave amplitude $F(\omega, \mu^2)$, given by eq. (37). Both λ and ν are positive provided that ω, the Regge trajectory, is positive. Using the differential property of the confluent hypergeometric function [10],

$$\frac{\partial}{\partial\nu}\Psi(a, c, ; \nu) \;=\; -a\Psi(a, c+1; \nu) \tag{44}$$

$F(\omega, \mu^2)$ becomes

$$F(\omega, \mu^2) \;=\; 8\pi^2\omega\frac{\lambda\Psi(1-\lambda, 1; \nu)}{\Psi(-\lambda, 0; \nu)} \tag{45}$$

$\Psi(a, c; \nu)$ is a many-valued function of ν, and we usually take its principal branch in the plane cut along the negative real axis. Therefore, $\Psi(a, c; \nu)$ is analytic for $\nu > 0$. For $\nu > 0$, the singularity of $F(\omega, \mu^2)$ must be the zeros of $\Psi(-\lambda, 0; \nu)$. $\Psi(a, c; \nu)$ cannot have positive zeros if $a > 0$ or $1 + a - c > 0$ [10]. This implies that $1 < \lambda$ must

be true for $\Psi(-\lambda, 0; \nu)$ to have positive zeros. From the definition of λ, $\lambda \sim 1/\omega$, where ω_{max} corresponds to $\lambda = 1$, and Ψ has one zero. Actually, according to Ref [10], the range $1 \leq \lambda < 2$, $\Psi(-\lambda, 0; \nu)$ has one zero. This can be seen by noting that [10]

$$\Psi(-n, c; \nu) = n!(-1)^n L_n^{c-1}(\nu) \tag{46}$$

where $L_n^{\mu}(\nu)$ is the generalized Laguerre polynomial [11]. Therefore

$$\begin{aligned} \Psi(-1, 0; \nu) &= (-1)L_1^{-1}(\nu) \\ &= \nu \end{aligned} \tag{47}$$

as $L_n^{-n}(\nu) = (-\nu)^n/n!$. The zero of $\Psi(-1, 0; \nu)$ is at $\nu = 0$ which in turn gives $\alpha_s \to \infty$ as $\omega = \omega_{max} = a_0/(8\pi^2 b) = 0.32$ is fixed by $\lambda = 1$. For $\lambda = 2$, which means $\omega = \omega_{max}/2 = 0.16$,

$$\Psi(-2, 0; \nu) = -\nu(2 - \nu) \tag{48}$$

where $L_2^{-1}(\nu) = -\nu(2 - \nu)/2$ is used. Both $\nu = 0$ and $\nu = 2$ are the zeros of $\Psi(-2, 0; \nu)$, $\nu = 2$ corresponding to $\alpha_s = \omega_{max}/(16\pi b) = 0.12$. The $\nu = 0$ solution is the subleading trajectory and so we do not consider here. Hence, from $\lambda = 1$ to $\lambda = 2$, α_s ranges from 0.12 to ∞ which covers a large range of the interesting physical region.

From the above discussion, we see that interesting physics already lies inside the range $1 \leq \lambda \leq 2$. λ is of order 1, so it is not very large. Neverthless, let us take a

large λ limit and compare the $\omega(\alpha_s)$ obtained with the exact results at $\alpha_s = \infty$ and $\alpha_s = 0.12$.

When $\lambda \to \infty$, $\Psi(-\lambda, 0; \nu)$ can be approximated as [10]

$$\Psi(-\lambda, 0; \nu) \simeq 2^{1/2} \lambda^{\lambda - 1/4} \nu^{-1/4} \, e^{\nu/2 - \lambda} \cos(\lambda\pi - 2(\lambda\nu)^{1/2} - \frac{\pi}{4}), \tag{49}$$

which in turn gives

$$F(\omega, \mu^2) = 8\pi^2 \omega [-\frac{1}{4\nu} + \frac{1}{2} + (\frac{\lambda}{\nu})^{1/2} \tan(\lambda\pi - 2(\lambda\nu)^{1/2} - \frac{1}{4})]. \tag{50}$$

The first two terms can be dropped as they contribute nothing to the scattering amplitude after performing the Mellin transformation. From Eq. (50), we see that $F(\omega, \mu^2)$ has pole singularities at

$$\lambda\pi - 2(\lambda\nu)^{1/2} - \frac{1}{4}\pi = \frac{n}{2}\pi, \tag{51}$$

where the leading trajectory corresponds to $n = 1$,

$$\begin{aligned} \omega_{run}(\alpha_s) &= \frac{\omega_{max}}{[\frac{3}{4} + \frac{2}{\pi}(\frac{\omega_{max}}{4\pi b \alpha_s})^{1/2}]} \\ &= \frac{\omega^+}{[\frac{4}{\pi} + \frac{6\pi^2 b}{a_0}\omega^+]}. \end{aligned} \tag{52}$$

When $\alpha_s = \infty$, $\omega_{run} = 4\omega_{max}/3$ which is 33% larger than the exact value. For $\alpha = \omega_{max}/(16\pi b) = 0.12$, $\omega_{run} = 0.99\omega_{max}/2$, which is only 1% off. The above analysis indicates that the ω_{run} obtained from the large λ approximation is accurate in the region where the running coupling is small. Equation (52) shows that the trajectory of

the mesonic Reggeon is highly non-linear in α_s, and one can see that $\omega_{run}(\alpha_s)$ is always less than $\omega^+(\alpha_s)$. The singularity of the partial wave amplitude in running coupling moves to the left of that of fixed coupling. For $\alpha_s = 0.20$, a typical value, $\omega_{run} = 0.19$ which is less than half of $\omega^+ = 0.40$. The smallness of the mesonic Reggeon trajectory imposes a serious problem of observing the mesonic exchange in the parton level experimentally, especially given that the mesonic exchange amplitude is already suppressed by a factor of s relative to the Pomeron exchange which constitutes a strong background.

The amplitude can be obtained by the Mellin transforming Eq. (50),

$$M^+_{run}(s) \;\; = \;\; 64\pi^3\omega^2_{run} b(\frac{\alpha_s}{2\pi a_0})^{1/2}\, e^{\omega_{run} y}. \tag{53}$$

There is no justification for the correctness of the above expression in large λ approximation, although the trajectory does give fairly accurate results. Therefore, it is natural to consider the numerical evaluation of the amplitude and to compare it with the approximated result obtained in this section. To our surprise, the formula (53) is accurate to within 10%, as will be shown in the next section.

4.3 Numerical Calculation

Let us begin the numerical calculation by performing the Mellin transformation on $F(\omega, \mu^2)$ using the expression (45). This leads to

$$\begin{aligned} M^+_{run} &= \int \frac{d\omega}{2\pi i} (\frac{-s}{t})^\omega \, 8\pi^2\omega \, \frac{\lambda\Psi(1-\lambda,1;\nu)}{\Psi(-\lambda,0;\nu)} \\ &= 8\pi^2\omega \, (\frac{-s}{t})^\omega \, n(\alpha_s) \mid_{\omega=\omega_R} \end{aligned} \tag{54}$$

with

$$n(\alpha_s) = \frac{g^2 b}{1 + \frac{g^2 b}{\omega\Psi(1-\lambda,1;\nu)} \frac{d\Psi(\lambda,0;\nu)}{d(-\lambda)}} \mid_{\omega=\omega_R} \tag{55}$$

where ω_R, the leading trajectory, is the root of $\Psi(-\lambda, 0; \nu)$. We are interested in the range $1 \leq \lambda \leq 2$. The roots $\omega_R(\alpha_s)$ in this range are shown in Fig. 4. The large λ approximation suggests that we use the following parameterization to fit the data in Fig.4, where α and β are constants:

$$\omega_R(\alpha_s) = \frac{\omega_{max}}{\alpha + \beta\alpha_s^{-1/2}} \tag{56}$$

Numerical fitting gives

$$\alpha = 1.14 \times \frac{3}{4}, \text{ and} \qquad \beta = 0.90 \times \frac{2}{\pi}(\frac{\omega_{max}}{4\pi b})^{1/2} \tag{57}$$

when we use the data from $1.5 \leq \lambda \leq 2$ corresponding to $0.121 \leq \alpha_s \leq 0.382$. Compared with $\alpha = 3/4$ and $\beta = \frac{2}{\pi}(\frac{\omega_{max}}{4\pi b})^{1/2}$ in large λ approximation, it once again confirms that it is a good approximation for the trajectory ω_R.

For the normalization $n(\alpha_s)$, the results for $\alpha_s = 0.121$ to 0.382 are shown in Fig. 5. They can be summarized by the following formula:

$$n(\alpha_s) \;=\; 0.8958\pi b\,\omega_R(\frac{\alpha_s}{2\pi a_0})^{1/2}, \tag{58}$$

where $\omega_R(\alpha_s)$ is given by Eq. (56). Therefore,

$$M^+_{run}(s) \;=\; 0.895\times 64\pi^3 b\,\omega_R^2(\frac{\alpha_s}{2\pi a_0})^{1/2}e^{\omega_R y} \tag{59}$$

is our final result for the positive signature mesonic singlet exchange in the t channel. The factor 0.895 indicates that the large λ approximation has a 10% error in the normalization $n(\alpha_s)$.

5 Conclusion

In this paper we analyze the scattering amplitudes of quarks and anti-quarks through flavour exchange in the Regge limit. Both the normalization factors and the mesonic Reggeon trajectory are obtained.

The negative and positive signatures of the fixed coupling constant case give nearly the same energy behavior at the SSC energies. The Regge trajectories are porportional to $\sqrt{\alpha_s(-t)}$ which are non-linear in strong coupling constant.

The inclusion of the effect of the running coupling constant reduces the magntiude of the amplitudes dramatically. The failure of small b expansion indicates that the

running coupling effect is not a small perturbation relative to the fixed coupling case. The change of the nature of singularty, from a square root branch cut to a simple pole, reflects the importance of the effect of the running coupling constant. Moreover, the position of the singularity shifts to the left and is a lot smaller than that of the fixed coupling case. Its smallness imposes a serious challange to observing experimentally the mesonic exchange in the parton level.

Although in this paper we study just the positive signature in the running coupling case, as explained in Sec. 4, we do expect that positive and negative signature amplitudes have approximated normalization factors and trajectories. This enables us to make an estimation on the possibility of observing mesonic exchange in the parton level.

Acknowledgements

I am very much indebted to Professor A.H.Mueller for suggesting this work and for many stimulating discussions. I am also indebted to Stanley Brodsky for constructive comments on an earlier draft of this paper.

References

[1] B. Badelek, K. Charchula, M. Krawczyk and J. Kwiecinski, Rev. of Mod. Phys. 64 (1992) 927

[2] A.H. Mueller and H. Navelet, Nucl. Phys. B282 (1987) 727

[3] W.-K. Tang, Phys. Lett. B278 (1992) 363

[4] J. Kwiecinski, A.D. Martin and P.J. Sutton, Phys. Lett. B287 (1992) 254 and Phys. Rev. D46 (1992) 921

[5] J. Bartels, A. De Roeck and M. Loewe, Z. Phys. C54 (1992) 635

[6] J. Bartels, M. Besancon, A. De Roeck and J. Kurzhoefer, DESY Preprint (1992)

[7] A.H. Mueller and W.-K. Tang, Phys. Lett. B284 (1992) 123

[8] R. Kirschner, Z. Phys. C31(1986) 135 and references therein

[9] R. Kirschner and L.N. Lipatov, Sov. Phys. JETP 56 (1982) 266 and Nucl. Phys. B213 (1983) 122

[10] H. Bateman, Higher Transcendental Functions V.1 (McGraw-Hill, 1953)

[11] W. Magnus, F. Oberhettinger and R.D. Soni, Formulas and Theorems for the Special Functions of Mathematical Physics, 3rd edition (Springer-Verlag 1966)

Figure Captions

Fig. 1: Elastic quark anti-Quark annihilation.

Fig. 2: The square-root branch cut of f_0^+. C is the contour of the Mellin transformation which lies to the right of the singularities.

Fig. 3: The square-root branch cut of f_0^-.

Fig. 4: Numerical solution (dot) of the Regge trajectory ω_R as function of strong coupling constant α_s. The solid line is the numerical fitting given by eqs. (56, 57).

Fig. 5: Normalization factor $n(\alpha_s)$ from $\alpha_s = 0.121$ to 0.382

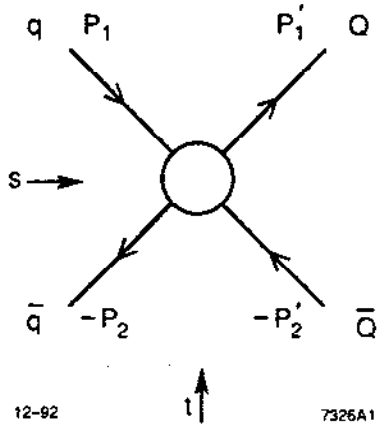

Fig. 1

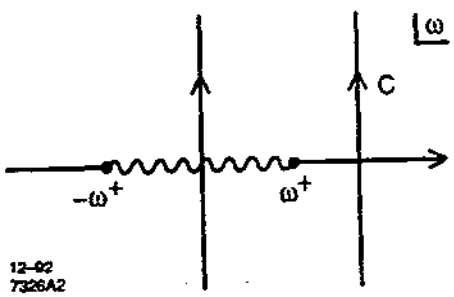

Fig. 2

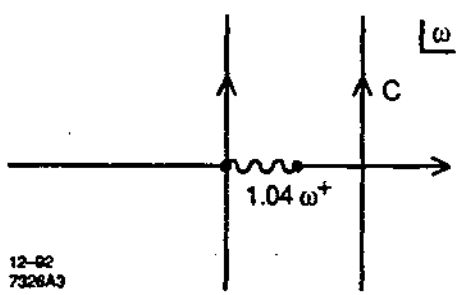

Fig. 3

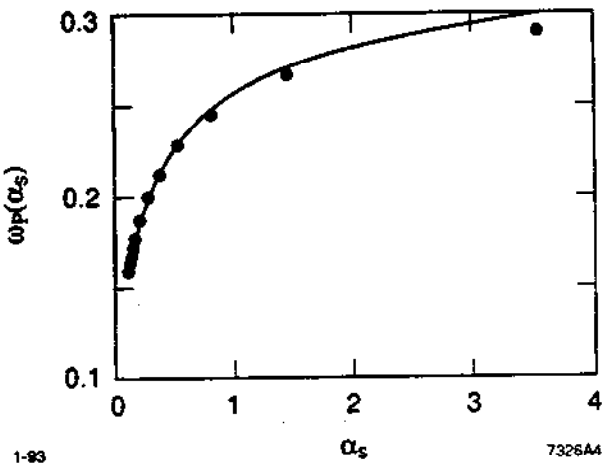

Fig. 4

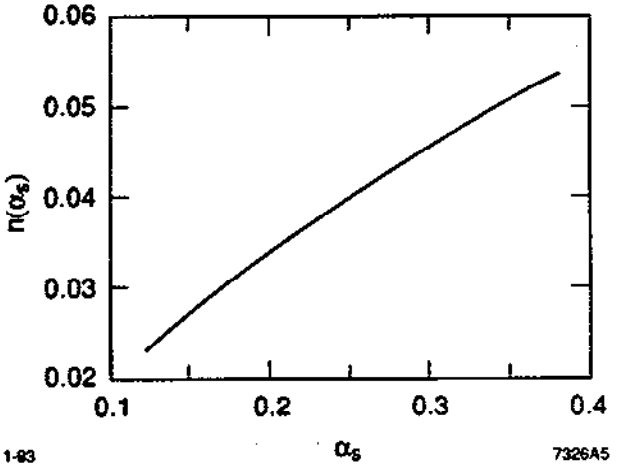

Fig. 5

SLAC–PUB–6024
February 1993
(T)

ERRATA

HIGH ENERGY QUARK–ANTIQUARK ELASTIC SCATTERING WITH MESONIC EXCHANGE*

WAI-KEUNG TANG

Stanford Linear Accelerator Center

Stanford University, Stanford CA 94309 USA

Page 19: *Equation 51 and the line following should read:*

$$\lambda\pi - 2(\lambda\nu)^{1/2} - \frac{1}{4}\,\pi \;=\; \frac{n}{2}\,\pi\;, \tag{51}$$

where the correct solution corresponds to $n = 1$. The trajectory is

Page 20: *Equation 53 should read:*

$$M^{+}_{run}(s) \;=\; 64\,\pi^3\,\omega^2_{run}\,b\left(\frac{\alpha_s}{2\pi a_0}\right)^{1/2} \quad \exp\{\omega_{run}\,y\}\;. \tag{53}$$

Page 21: *Equation 59 should read:*

$$M^{+}_{run}(s) \;=\; 0.895\times 64\,\pi^3\,b\,\omega^2_R(\alpha_s)\left(\frac{\alpha_s}{2\pi a_0}\right)^{1/2} \quad \exp\{\omega_R(\alpha_s)\,y\} \tag{59}$$

Submitted to Nuclear Physics B

*Work supported by Department of Energy contracts DE–AC03–76SF00515.

SLAC–PUB–6024
February 1993
(T)

ERRATA

HIGH ENERGY QUARK–ANTIQUARK ELASTIC SCATTERING WITH MESONIC EXCHANGE*

WAI-KEUNG TANG

Stanford Linear Accelerator Center
Stanford University, Stanford CA 94309 USA

Page 19: *Equation 51 and the line following should read:*

$$\lambda\pi - 2(\lambda\nu)^{1/2} - \frac{1}{4}\,\pi \;=\; \frac{n}{2}\,\pi\;, \tag{51}$$

where the correct solution corresponds to $n = 1$. The trajectory is

Page 20: *Equation 53 should read:*

$$M^{+}_{run}(s) \;=\; 64\,\pi^3\,\omega^2_{run}\,b\left(\frac{\alpha_s}{2\pi a_0}\right)^{1/2} \quad \exp\{\omega_{run}\,y\}\;. \tag{53}$$

Page 21: *Equation 59 should read:*

$$M^{+}_{run}(s) \;=\; 0.895\times 64\,\pi^3\,b\omega^2_R(\alpha_s)\left(\frac{\alpha_s}{2\pi a_0}\right)^{1/2} \quad \exp\{\omega_R(\alpha_s)\,y\} \tag{59}$$

Submitted to Nuclear Physics B

*Work supported by Department of Energy contracts DE–AC03–76SF00515.